Piotr Noga, Marek Węglowski, Patrycja Zimierska-Nowak, Maria Richert, Jerzy Dworak, Janusz Rykała

Influence of welding techniques on microstructure and hardness of steel joints used in automotive air conditioners

Wpływ technologii spawania na mikrostrukturę oraz twardość złączy stalowych wykorzystywanych w klimatyzatorach samochodowych

Abstract

Austenitic steels belong to a group of special-purpose steels that are widely used in highly aggressive environments due to their enhanced anticorrosive behavior and high mechanical properties. The good formability and weldability of these materials has made them very popular in automotive AC systems. This study presents the results of hardness tests and microstructure observations on plasma- and laser-welded joints. The examined joints consisted of two different stainless steel components; i.e., a nipple made from corrosion-resistant AISI 304 steel and a corrugated hose made from 316L steel. Microplasma welding was carried out on a workstation equipped with an MSP-51 plasma supply system and a BY-100T positioner. The laser-welded joint was made on a numerically controlled workstation equipped with an Nd:YAG laser (without filler material) with 1 kW of maximum power; the rotational speed of the welded component was $n = 4$ rpm. Microstructural observations were performed using a scanning electron microscope and an optical microscope. Vickers hardness was measured with a hardness tester. The obtained results proved that both the microplasma- and laser-welded joints were free from any visible welding imperfections. In the micro areas of the austenitic steel weld, crystals of intercellular ferrite appeared against a background of austenite. The crystallization front (depending on the welding technology) was running from the fusion line towards the weld axis. The grain size depended on the distance from the fusion line.

Keywords: laser welding, microplasma welding, elements of automotive air conditioners, delta ferrite

Piotr Noga M.Sc. Eng.: AGH University of Science and Technology, Faculty of Non-Ferrous Metals, Krakow, Poland, **Marek Węglowski Ph.D., Jerzy Dworak M.Sc., Janusz Rykała M.Sc.:** Institute of Welding, Gliwice, Poland, **Patrycja Zimierska-Nowak M.Sc.:** Boryszew S.A. MAFLOW Branch in Tychy, Chełmek, Poland, **Maria Richert D.Sc. Ph.D. Eng.:** AGH University of Science and Technology, Faculty of Management, Krakow, Poland; pionoga@agh.edu.pl

Streszczenie

Stale austenityczne należą do grupy stali specjalnych, szeroko stosowanych w silnie agresywnych środowiskach ze względu na swoje doskonałe właściwości antykorozyjne oraz mechaniczne. Dodatkowo z uwagi na ich bardzo dobrą zdolność do odkształceń plastycznych oraz spawalność mają zastosowanie w samochodowych układach klimatyzacyjnych.

W pracy przedstawiono wyniki badań twardości oraz badań metalograficznych mikrostrukturalnych złączy spawanych łukiem plazmowym oraz wiązką laserową. Łączony element składał się z różnoimiennych stali nierdzewnych: tulei wykonanej ze stali odpornej na korozję AISI 304 oraz mieszka sprężystego wykonanego ze stali odpornej na korozję AISI 316L. Spawanie plazmowe przeprowadzono na stanowisku wyposażonym w zasilacz plazmowy MSP-51 oraz obrotnik typu BY-100T. Złącza spawane laserowo wykonano na specjalnym stanowisku sterowanym numerycznie za pomocą lasera typu Nd:YAG bez materiału dodatkowego, o maksymalnej mocy 1 kW oraz prędkości obrotowej elementu spawanego n = 4 obr/min. Obserwacje mikroskopowe przeprowadzono na skaningowym mikroskopie elektronowym oraz optycznym mikroskopie świetlnym, natomiast twardość mierzono twardościomierzem SHIMADZU HMV-G. Na podstawie wyników badań stwierdzono, że w spoinach uzyskanych zarówno w technice spawania plazmowego, jak i laserowego nie zaobserwowano niezgodności spawalniczych, a w mikroobszarach stali austenitycznej, w spoinie, występują kryształy międzykomórkowego ferrytu na tle austenitu. Ponadto wykazano, że front krystalizacji (w zależności od technologii spawania) występuje od linii wtopienia w kierunku osi spoiny. Zaobserwowano również, że wielkość ziarna jest zależna od odległości od linii wtopienia.

Słowa kluczowe: spawanie laserowe, spawanie plazmowe, elementy kilmatyzacji samochodowej, ferryt delta

1. Introduction

Parts of automotive air conditioners must be joined together. Typically, the components of air conditioners are made from steel, polymer materials, or aluminum alloys. Prospects of future use have AISI 304 and AISI 316L austenitic stainless steels offering not only satisfactory corrosion resistance but also high deformability and weldability. Owing to these properties, they have already found wide application in many sectors of the industry [1–3]. The main welding technologies used in the automotive industry include resistance welding, laser beam welding, arc welding, braze welding, and also – though applied only occasionally – the FSW (Friction Stir Welding) process [4–5]. Among the available welding technologies, laser beam welding is gaining widespread popularity. This process is characterized by a number of favorable features, to mention only high energy density, small width of HAZ, high welding speed, and small deformation of the welded elements [6]. Besides laser beam welding, other alternative welding technologies used for joining austenitic steels include microplasma welding (among others), which are particularly useful for thin-walled products [7–8]. Microplasma welding is based on the traditional TIG welding method [9]. It allows us to make high-quality welded joints in one pass and is used in the aerospace, chemical, petrochemical, and machine building industries [10–12].

The aim of this study was to conduct metallographic examinations of welds made by the laser beam technique and microplasma welding by using light microscopy and SEM for these examinations. As part of the research, the hardness of the welded joints was also measured.

2. Research methodology

Tests were carried out on butt joints made from dissimilar corrosion-resistant steels. The nipple was made from AISI 304 (Fig. 1b), and the corrugated hose from AISI 316L (Fig. 1a). The diameter of the welding spot was 10 mm. The chemical composition of the welded steel components is shown in Table 1. Technological trials of microplasma welding were carried out at the Institute of Welding in Gliwice on a workstation equipped with an MSP-51 plasma supply unit and a BY-100T-type positioner. The welded components were fixed in the positioner, and tooling specially designed for this purpose was used (Fig. 2). The plasma holder was positioned directly above the rotating welded component.

The following process parameters were applied in the plasma arc-welding test: rotational speed 3 rpm, current intensity $I = 8.5-8.6$ A, arc voltage $U = 22.5$ V, plasma gas 100% Ar, flow rate 0.3 1/min, shielding gas 97% Ar + 3% H_2, and flow rate 6.0 l/min.

The laser beam welding was carried out on a special numerically controlled workstation using the Nd: YAG laser and the following welding process parameters: pulse shaping CrNi pulse type, maximum pulse power $P = 1000$ W, pulse duration $t = 4$ ms, laser beam diameter 0.6 mm, rotational speed of the welded component $n = 4$ rpm, pulse repetition frequency $f = 10.45$ Hz, laser head positioning place – contact point between welded components, shielding gas Ar, and flow rate 10 l/min.
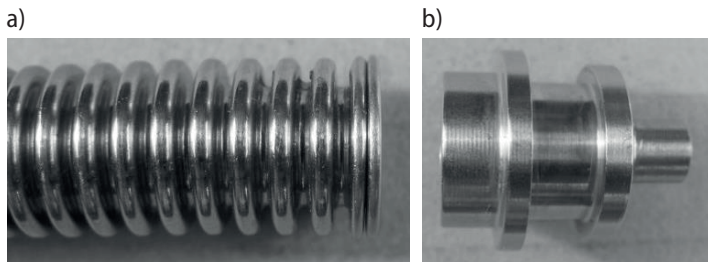
a)   b)

Fig. 1. Welding elements: a) corrugated hose; b) nipple

Table 1. Chemical composition of tested materials, wt.%

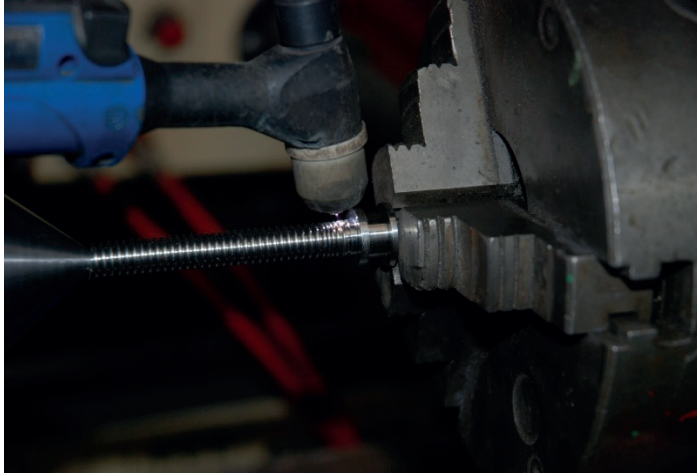| Material	Cr	Ni	Mo	C	Si	Mn	P	S	N	Fe
AISI316L	16.6	10.5	2.02	0.033	0.42	0.92	0.038	<0.001	0.013	rest
AISI304	17.50–19.50	8.00–10.50	–	<0.07	<1.0	<2.0	<0.045	<0.015	<0.11	rest

Fig. 2. General view of MSP-51 microplasma arc welding machine and workstation with tooling

Microscopic observations were performed using a Hitachi SU70 scanning electron microscope and an Olympus GX51 optical light microscope. Hardness measurements were made with a SHIMADZU HMV-G hardness tester under a load of HV 0.5.

3. Test results and discussion

The structures of the laser-welded joint composed of a nipple (AISI 304) and the corrugated hose (AISI 316L) are shown in Figure 3. Both types of steel (AISI 316L and AISI 304) in areas outside the welding zone are characterized by the presence of equiaxed austenite grains with straight-line boundaries and characteristic annealing twins. Twins typically occur in the structure of metals with an FCC lattice and low stacking fault energy, and both of the tested steels possess these features. In the corrugated hose made from AISI 316L steel, the mean grain diameter determined by the planimetric method is 9 μm, while in the nipple made from AISI 304 steel, it is 22 μm. The corrugated hose also shows the presence of narrow bands characteristic of δ ferrite. Microscopic examinations of the laser-welded joint proved the correct formation of the weld face, characterized by the proper penetration and fusion without any cracks, blistering, or inclusions. The joint area has a diverse microstructure resulting from different solidification rates of the welded materials. It should be noted that laser welding was carried out with a pulse beam. In Figure 3, areas of the impact of individual pulses are visible. The micro area in Figure 3d shows the presence of columnar grains that crystallize in the direction from the fusion line towards the weld axis. Figure 3c shows the microstructure of the weld zone directly adjacent to the AISI 304 steel with joint lines well-visible between the nipple

and the weld, while the microstructure of a weld-AISI 316L corrugated hose interface is illustrated in Figure 3e. In both cases, the boundaries are clearly marked, and it is easy to notice the occurrence of intercellular δ ferrite resting against the austenite background.
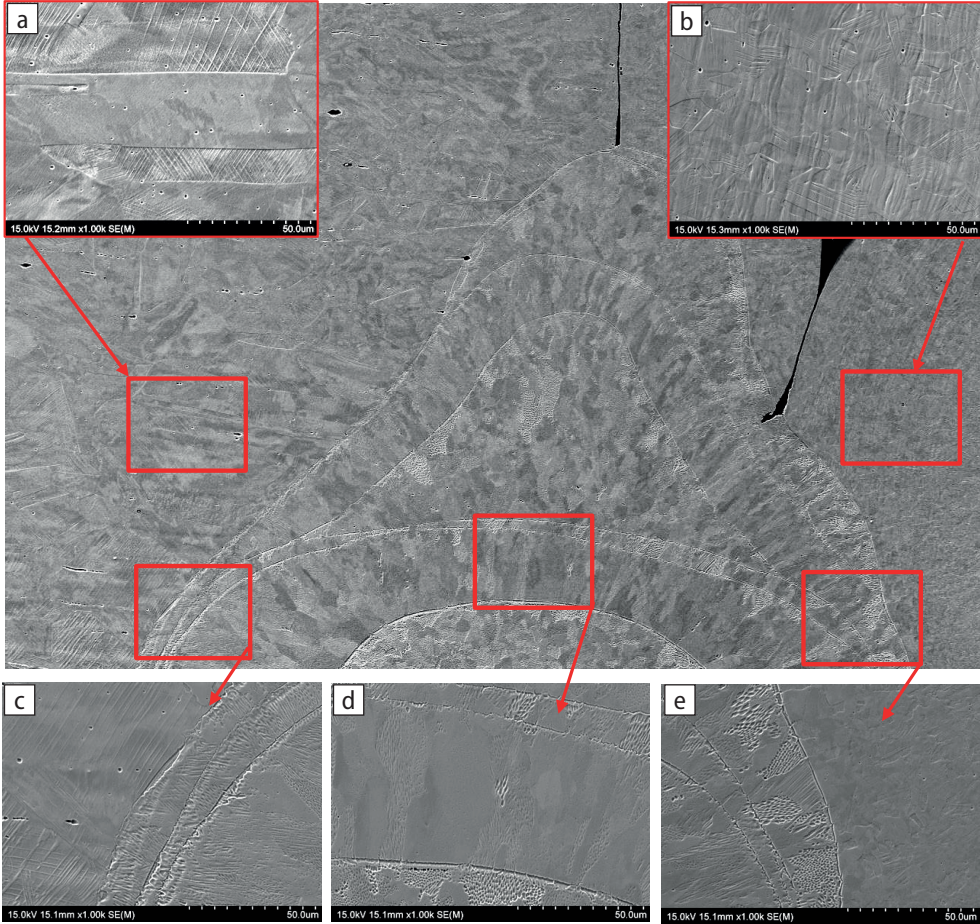

Fig. 3. Microstructure of laser beam welded joint: a) base material AISI 304; b) base material AISI 316L; c) microstructure of a weld-AISI 304; d) the microstructure of columnar grains; e) microstructure of a weld-AISI 316L

The structure of the joint made by microplasma welding is shown in Figure 4. As in the case of laser welding, this joint is also free from any welding incompatibilities – a fact that indicates well-chosen welding process parameters. Compared with the laser-welded joint, the joint made by the microplasma technique has a more-uniform structure throughout the entire volume of the weld. Figure 4a shows the central part of the joint; Figure 4c shows the boundary area of the weld adjacent to the AISI 316L steel (corrugated hose),

while the boundary area adjacent to the AISI 304 steel (nipple) is shown in Figures 4b, 4d, and 4e. An examination of the joint microstructure revealed crystals of intercellular ferrite resting against an austenite background. In the vicinity of the base material, these crystals show a parallel array, (however, losing this clear orientation towards the joint surface). The occurrence of δ ferrite in the area of the welded joint made by both techniques of the laser and microplasma welding can be explained by fast cooling after the welding process, during which an incomplete phase transformation $\delta \rightarrow \gamma$ (δ-ferrite, γ-austenite) takes place. The result is a non-equilibrium structure and increased content of δ ferrite in this structure [13–16]. A small amount of δ ferrite is desirable to avoid the problem of hot cracking during welding [17, 18]; however, excessively high amounts of this constituent can lead to microsegregations and the formation of areas poor in chromium, which deteriorate the corrosion resistance due to the less-stable passive film they tend to form.
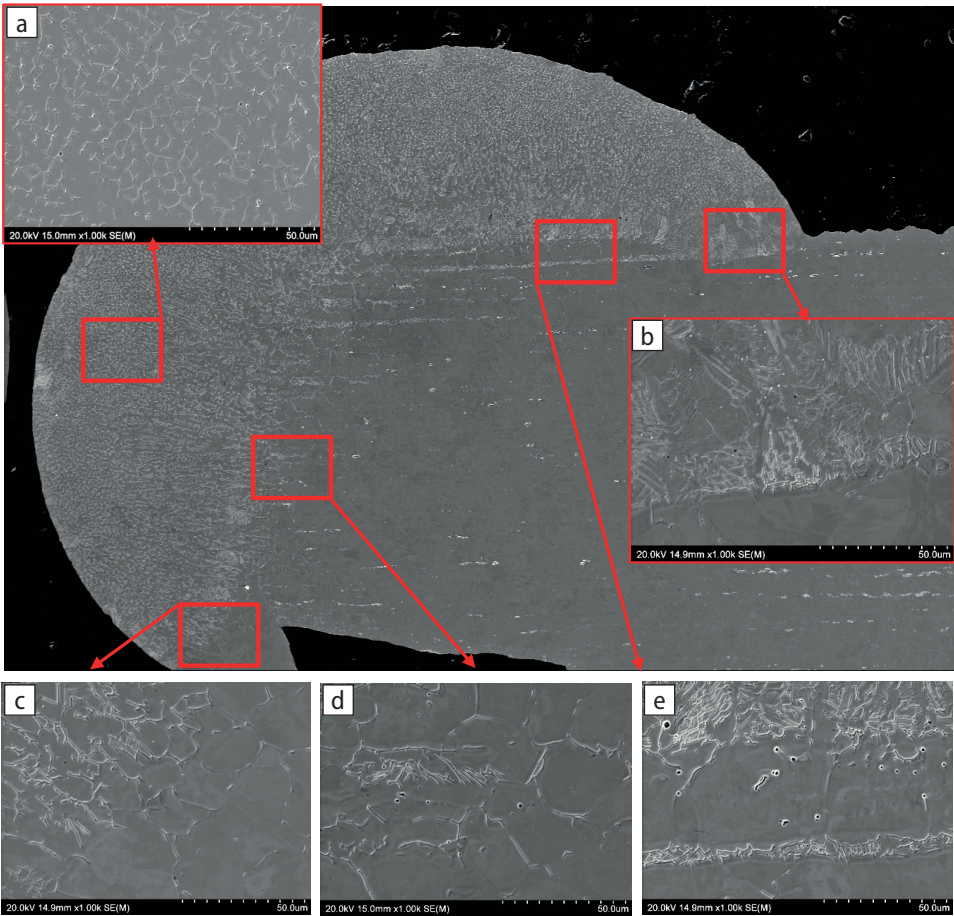

Fig. 4. Microstructure of microplasma-arc-welded joint: a) microstructure of central part the joint; c) microstructure of a weld-AISI 316L; (b, d ,e) microstructure of a weld-AISI 304

Figures 5 and 6 show the results of the hardness measurements and locations of these measurements in the laser-welded joint and plasma-welded joint, respectively. In both welds, a drop in hardness was observed, from an average of 300 HV in the area of the parent metal to about 210 HV in the area of the laser-welded joint and from an average of 270 HV in the area of the parent metal to about 200 HV in the area of the plasma-welded joint. In percentages, the drop in the hardness value is approximately 30% for both of the welding methods. The higher hardness recorded in the corrugated hose sample is probably due to the difference in chemical composition and higher cold work during plastic forming. A similar situation with higher hardness in the case of the nipple made of AISI304 is also a result of plastic deformation.
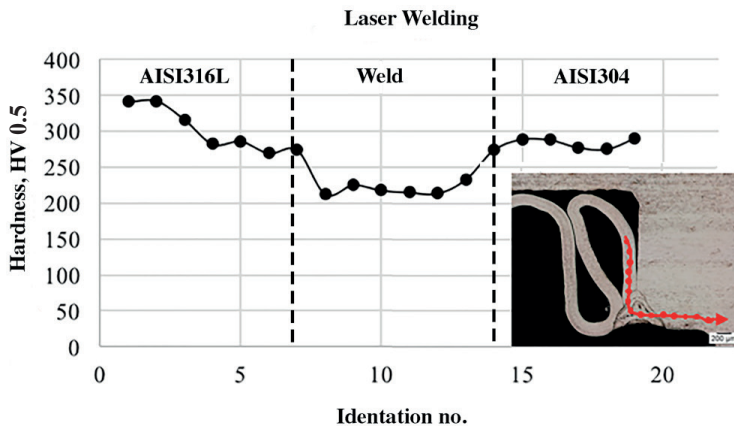

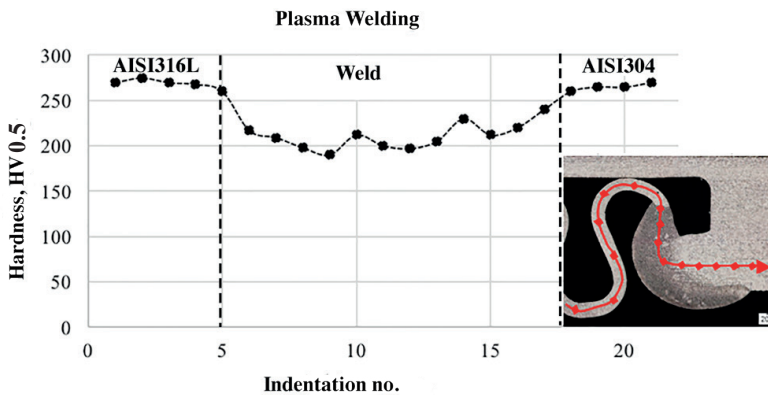Fig. 5. Hardness profile on cross-section of laser-welded specimens

Fig. 6. Hardness profile on cross-section of microplasma-welded specimens

287

In the corrugated hose made from 316L steel, the decrease in hardness in the direction towards the joint can be due to a coarse-grain structure obtained under the influence of welding heat. In both cases, the reduced hardness of the weld can be explained by the differences in the microstructure of the weld and parent metal. The lower hardness value is most likely caused by a higher fraction of the stable γ phase accompanied by a lower content of the δ phase [16].

Studies allowed for a quality assessment of the welded joints in terms of both the microstructure and mechanical properties. Visual and metallographic examinations confirmed the correct workmanship of the joints made by laser beam welding and microplasma arc welding despite some significant differences in the thickness of the corrugated hose (about 200 μm) and nipple. Examinations of the welded joint microstructure revealed the presence of crystals of intercellular ferrite visible against a background of austenite. As follows from the authors' research [19–21], the functional properties of joints welded from austenitic steel depend to a large extent on the content of δ ferrite, which is formed in the incomplete $\delta \rightarrow \gamma$ phase transformation caused by rapid cooling after the welding process [22]. In industrial welded structures, the occurrence of δ ferrite in the joint area is desirable, as it increases the resistance of welds to hot cracking and promotes refinement of the weld microstructure. The harmful effect of the presence of δ ferrite is the reduced corrosion resistance of the welded joints due to the appearance of areas poor in chromium and the formation of a less-stable passive film [21, 23–25]. The amount of δ ferrite in the microstructure of the austenitic steel joints depends not only on the content of austenite-forming elements (Ni, N, C, Mn) and ferrite-forming elements (Cr, Mo, Si, W) but also on the technological factors such as the welding current, welding speed, and linear welding energy, all of which affect the $\delta \rightarrow \gamma$ transformation through heat dissipation [26, 27]. All of these parameters determine the amount of retained δ ferrite in the austenitic matrix (mainly in the form of dendrites), since the $\delta \rightarrow \gamma$ transformation is a diffusion-controlled process. In laser-welded joints, the percent volume fraction of δ ferrite (calculated by a metallographic method using the ImageJ software) amounted to 30%. The amount of δ ferrite obtained in the joints welded by the microplasma process was 39%. This difference results from the different linear energy of the welding methods used. Rapid cooling after the welding process (especially of thin-walled components such as the corrugated hose) does not provide sufficient time for a complete phase transformation.

4. Conclusions

Based on the results of the conducted research, the following conclusions were drawn.
– Both laser and microplasma welding produced joints free of welding incompatibilities.
– Columnar grains crystallizing from the fusion line towards the weld axis and δ ferrite visible against an austenite background were present in the weld zone made by the process of laser beam welding.

- In the joint made by plasma arc welding, the distribution and amount of δ ferrite (30 vol% in laser-welded joints and 39 vol% in plasma-welded joints) assumed different values and configurations depending on the distance from the parent metal; this effect was due to the rate of heat dissipation from the weld.
- The hardness of the welded joint was inferior to the hardness of the parent metal; a probable source of this effect is to be searched in a higher content of the stable γ phase accompanied by a lower content of the δ ferrite.

Acknowledgements

References

[1] Méndez C.M., Covinich M.M., Ares A.E.: Resistance to Corrosion and Passivity of 316L Stainless Steel Directionally Solidified Samples. In: Aliofkhazraei M., Developments in Corrosion Protection. InTech 2009, 41–63

[2] Ziętala M., Durejko T., Polański M., Kunce I., Płociński T., Zieliński W., Łazińska M., Stępniowski W., Czujko T., Kurzydłowski K.J., Bojar Z.: The microstructure, mechanical properties and corrosion resistance of 316 L stainless steel fabricated using laser engineered net shaping. Materials Science and Engineering A, 677, November (2016), 1–10

[3] Zhou L., Nakata K., Tsumura T., Fujii H., Ikeuchi K., Michishita Y., Fujiya Y., Morimoto M.: Microstructure and Mechanical Properties of 316L Stainless Steel Filling Friction Stir-Welded Joints. Journal of Materials Engineering and Performance, 23, 10 (2014), 3718–3726

[4] Węglowski M.S., Stano S.: Właściwości złączy spawanych laserowo ze stali HDT580X. Archiwum Technologii Maszyn i Automatyzacji, 29, 1 (2009), 268–273

[5] Hong K.-M., Shin Y.C.: Prospects of laser welding technology in the automotive industry: A review. Journal of Materials Processing Technology, 245 (2017), 46–69

[6] Mackwood A.P., Crafer R.C.: Thermal modelling of laser welding and related processes: A literature review. Optics & Laser Technology, 37, 2 (2005), 99–115

[7] Prasad K.S., Rao C.S., Rao D.N.: Study on weld quality characteristics of microplasma arc welded austenitic stainless steels. Procedia Engineering, 97 (2014), 752–757

[8] Prasad K.S., Rao C.S., Rao D.N.: Effect of pulsed current microplasma arc welding process parameters on fusion zone grain size and ultimate tensile strength of SS304L sheets. International Journal of Lean Thinking, June 2012, 107–118

[9] Liu Z.M., Cui S.L., Luo Z., Zhang C.Z., Wang Z.M., Zhang Y.C.: Plasma arc welding: Process variants and its recent developments of sensing, controlling and modeling. Journal of Manufacturing Processes, 23 (2016), 315–327

[10] Martikainen J.K., Moisio T.J.I.: Investigation of the Effect of Welding Parameters on Weld Quality of Plasma-Arc Keyhole Welding of Structural-Steels. Welding Journal, 72, 7 (1993), S329–S340

[11] Martikainen J.: Conditions for achieving high-quality welds in the plasma-arc keyhole welding of structural steels. Journal o Materials Processing Technology, 52, 1 (1995), 68–75

[12] Wu C.S., Jia C.B., Chen M.A.: Control System for Keyhole Plasma Arc Welding of Stainless Steel Plates with Medium Thickness. Supplement to the Welding Journal, 89, November (2010), 225–231

[13] Hanninen H., Romu J., Ilola R., Tervo J., Laitinen A.: Effects of processing and manufacturing of high nitrogen-containing stainless steels on their mechanical, corrosion and wear properties. Journal of Materials Processing Technology, 117, 3 (2001), 424–430

[14] Yan J., Gao M., Zeng X.: Study on microstructure and mechanical properties of 304 stainless steel joints by TIG, laser and laser-TIG hybrid welding. Optics and Lasers in Engineering, 48, 4 (2010), 512–517

[15] Berretta J.R., de Rossi W., Neves M., Alves de Almeida I., Dias Vieira Junior N.: Pulsed Nd:YAG laser welding of AISI 304 to AISI 420 stainless steels. Optics and Lasers in Engineering, 45, 9 (2007), 960–966

[16] Kumar N., Mukherjee M., Bandyopadhyay A.: Comparative study of pulsed Nd:YAG laser welding of AISI 304 and AISI 316 stainless steels. Optics & Laser Technology, 88 (2017), 24–39

[17] Lo I.H., Tsai W.T.: Effect of heat treatment on the precipitation and pitting corrosion behavior of 347 SS weld overlay. Materials Science and Engineering A, 355, 1–2 (2003), 137–143

[18] Cui Y., Lundin C.D.: Evaluation of initial corrosion location in E316L austenitic stainless steel weld metals. Materials Letters, 59, 12 (2005), 1542–1546

[19] Pujar M.G., Dayal R.K., Gill T.P.S., Malhotra S.N.: Role of δ-ferrite in the dissolution of passive films on the austenitic stainless-steel weld metals. Journal of Materials Science Letters, 18, 10 (1999), 823–826

[20] Kumar N., Mukherjee M., Bandyopadhyay A.: Study on laser welding of austenitic stainless steel by varying incident angle of pulsed laser beam. Optics & Laser Technology, 94 (2017), 296–309

[21] Rho B.S., Hong H.U., Nam S.W.: Effect of δ-ferrite on fatigue cracks in 304L steels. International Journal of Fatigue, 22, 8 (2000), 683–690

[22] Wang X.N., Chen X.M., Sun Q., Di H.S., Sun L.N.: Formation mechanism of δ-ferrite and metallurgy reaction in molten pool during press-hardened steel laser welding. Materials Letters, 206 (2017), 143–145

[23] Ben Rhouma A., Amadou T., Sidhom H., Braham C.: Correlation between microstructure and intergranular corrosion behavior of low δ-ferrite content AISI 316L aged in the range 550–700°C. Journal of Alloys and Compounds, 708 (2017), 871–886

[24] Kina A.Y., Souza V.M., Tavares S.S.M., Pardal J.M., Souza J.A.: Microstructure and intergranular corrosion resistance evaluation of AISI 304 steel for high temperature service. Materials Characterization, 59, 5 (2008), 651–655

[25] Windyga A.: Redukowanie fazy ferrytycznej w spoinach stali austenitycznych. Wydawnictwa Przemysłu Maszynowego „WEMA", Warszawa 1984

[26] Chen Y.B., Lei Z.L., Li L.Q., Wu L.: Experimental study on welding characteristics of CO_2 laser TIG hybrid welding process. Science and Technology of Welding and Joining, 11, 4 (2006), 403–411

[27] Ciechacki K., Szykowny T.: Ocena jakości spawania różnoimiennych stali odpornych na korozję. Inżynieria i Aparatura Chemiczna, 5 (2010), 28–30